IOP Publishing Journal of Neural Engineering
J. Neural Eng. 12 (2015) 046006 (12pp) doi:10.1088/1741-2560/12/4/046006

Enhancing performances of SSVEP-based brain–computer interfaces via exploiting inter-subject information

Peng Yuan[1,4], Xiaogang Chen[1,4], Yijun Wang[2,3], Xiaorong Gao[1] and Shangkai Gao[1]

[1] Department of Biomedical Engineering, Tsinghua University, Beijing, 100084, People's Republic of China
[2] Swartz Center for Computational Neuroscience, Institute for Neural Computation, University of California, San Diego, La Jolla, CA 92093 USA
[3] State Key Laboratory on Integrated Optoelectronics, Institute of Semiconductors, Chinese Academy of Sciences, Beijing 100083, People's Republic of China

E-mail: gsk-dea@tsinghua.edu.cn (S Gao)

Received 7 December 2014, revised 29 March 2015
Accepted for publication 10 April 2015
Published 1 June 2015

Abstract

Objective. A new training-free framework was proposed for target detection in steady-state visual evoked potential (SSVEP)-based brain–computer interfaces (BCIs) using joint frequency-phase coding. *Approach.* The key idea is to transfer SSVEP templates from the existing subjects to a new subject to enhance the detection of SSVEPs. Under this framework, transfer template-based canonical correlation analysis (tt-CCA) methods were developed for single-channel and multi-channel conditions respectively. In addition, an online transfer template-based CCA (ott-CCA) method was proposed to update EEG templates by online adaptation. *Main results.* The efficiency of the proposed framework was proved with a simulated BCI experiment. Compared with the standard CCA method, tt-CCA obtained an 18.78% increase of accuracy with a data length of 1.5 s. A simulated test of ott-CCA further received an accuracy increase of 2.99%. *Significance.* The proposed simple yet efficient framework significantly facilitates the use of SSVEP BCIs using joint frequency-phase coding. This study also sheds light on the benefits from exploring and exploiting inter-subject information to the electroencephalogram (EEG)-based BCIs.

Keywords: Brain–computer interface (BCI), steady-state visual evoked potential (SSVEP) inter-subject information, template, online adaptation

(Some figures may appear in colour only in the online journal)

1. Introduction

Steady-state visual evoked potential (SSVEP)-based brain–computer interfaces (BCIs) have shown high performances in various BCI applications, such as spelling, device control and gaming etc [1–11]. As BCIs essentially are communication channels, more recently, multiple access (MA) methods in the telecommunications field have been introduced to design the SSVEP BCIs [8, 12–14]. A recent study on hybrid frequency and phase coding methods showed significantly improved BCI performance [14]. These kinds of SSVEP BCIs (hereafter named frequency-phase coding SSVEP BCIs) have the potential to implement BCI spellers with high information transfer rate (ITR) and have become one of the most state-of-the-art SSVEP BCI paradigms [14–17].

The challenge of target identification in frequency-phase coding SSVEP BCIs is to correctly recognize both the frequency and phase information of SSVEPs corresponding to a specific target among many candidates. Canonical correlation analysis (CCA) has been widely used to recognize frequency-

[4] Authors contributed equally to this paper.

coded targets in SSVEP BCIs due to its efficiency and training-free characters [7, 18]. However, CCA is not able to recognize the phase of SSVEPs. Besides, with short data length, CCA-based SSVEP detection can be easily deteriorated by spontaneous EEG activities. Therefore, the frequency-phase coding SSVEP BCIs require additional efforts. It has been confirmed that, to fully assess the frequency and phase features of SSVEPs, the key is to seek good SSVEP templates as the reference signals for CCA [14, 17]. Nakanishi *et al* [17] and Chen *et al* [14] proposed to use the average of multiple trials from individual training data as the reference signals (or template) and resort to an ensemble classifier to recognize targets. Although the proposed methods achieved significant accuracy improvement in comparison with the standard CCA method, the training-free character of CCA no longer holds. Note that in frequency-phase coding SSVEP BCIs, the number of targets is usually large (e.g. 40). For each target, multiple trials have to be collected and averaged to get a good template. Therefore, the training stage can be time-consuming and may give rise to visual fatigue, which hinders the practicality of BCIs in real-life applications. Hence, a method that can build a good template without relying on individual training data is desired. In addition, the EEG during operating BCIs is actually non-stationary due to the change of mental state and fatigue related issues [19–22]. The non-stationary problem would decay the algorithm and decrease BCI performance gradually. To alleviate the non-stationary problem, the online adaptation methods will be helpful [23–26].

Recently, studies on brain computing across multiple subjects have attracted growing attention in the BCI field. For instance, the studies in [27–31] proposed various extended common spatial pattern (CSP) algorithms to explore the inter-subject information for improving the performance of motor imagery-based BCIs. Kindermans *et al* [32] proposed to use a transfer learning approach to realize a zero-training BCI speller based on event-related potential (ERP). Wang *et al* [33] and Yuan *et al* [34, 35] proposed to integrate multiple subjects' EEGs to implement collaborative BCIs. The common goal of the above studies was to capture inter-subject information in order to improve BCI performance and reduce training time.

Inspired by these studies, we aimed to explore and exploit the inter-subject information to address the above problems in frequency-phase coding SSVEP BCIs. The contributions of this paper are as follows:

(1) A new training-free framework for target detection is proposed for frequency-phase coding SSVEP BCIs. The main idea is to transfer EEG templates from the existing subjects (named source subjects) to a new subject (named target subjects) to capture frequency and phase information of SSVEPs.
(2) Under this framework, a transfer template-based CCA (tt-CCA) method is first developed at the single-channel level and subsequently generalized to multi-channel conditions. Finally, an online transfer template method (ott-CCA) is further proposed to enable online adaptation of the templates.
(3) The efficiency of the proposed methods is proved by quantifying classification accuracy in an offline frequency-phase coding SSVEP BCI experiment. The significantly improved accuracy demonstrates the benefits from exploring and exploiting inter-subject information in the EEG to the implementation of BCIs.

The rest of this paper is organized as follows. Section 2 first describes the standard CCA methods, and then details the proposed methods including the tt-CCA method for single-channel and multi-channel conditions and the ott-CCA method for online adaptation. Section 3 describes the experimental settings. Section 4 illustrates the experimental results. Section 5 discusses important characteristics of the proposed methods and points out some directions for further improvement. Finally, section 6 concludes the study.

2. Methods

2.1. Standard CCA for SSVEP BCIs

Canonical correlation analysis (CCA) is a method of extracting similarity between two data sets [36]. CCA was first applied to SSVEP BCIs by Lin *et al* [18]. Therein, a time-consuming channel selection procedure was still needed in the training stage. Bin *et al* carried out another CCA-based method in an online BCI system where a fixed set of nine channels over the occipital cortex was used [7]. Since then, the CCA-based target identification method has been widely used in SSVEP BCIs. For convenience, the CCA algorithm proposed in [7] is referred to as standard CCA.

Let C, N, N_h, f_s denote the number of EEG channels, the number of time points, the number of harmonics being considered, and the sampling rate respectively. $X \in \mathbb{R}^{C\times N}$ is the multichannel EEG signal. $Y(f) \in \mathbb{R}^{2N_h\times N}$, termed the template (i.e. the reference signal; see equation (1)), is constituted by a set of sine and cosine signals with frequencies including the stimulus frequency f and its harmonics:

$$Y(f) = \begin{bmatrix} \cos(2\pi fn) \\ \sin(2\pi fn) \\ \vdots \\ \cos\left(2\pi N_h fn\right) \\ \sin\left(2\pi N_h fn\right) \end{bmatrix} \quad n = \frac{1}{f_s}, \frac{2}{f_s}, \cdots, \frac{N}{f_s} \tag{1}$$

Let $w_x \in \mathbb{R}^{C\times 1}$ and $w_y \in \mathbb{R}^{2N_h\times 1}$ denote weighting vectors for X and $Y(f)$, respectively. The idea of CCA is to find w_x and w_y that maximize the correlation between two one-dimensional variables x and y (termed the canonical variables, $x = w_x{}^T X$, $y = w_y{}^T Y(f)$). This is achieved by solving the

following optimization problem:

$$\max_{w_x, w_y} \rho(x, y) = \frac{E\left[w_x^T XY(f)^T w_y\right]}{\sqrt{E\left[w_x^T XX^T w_y\right] E\left[w_x^T Y(f) Y(f)^T w_y\right]}} \quad (2)$$

The optimization problem in equation (2) is equivalent to solving a generalized eigenvalue decomposition problem. This yields the maximum correlation $\rho(f)$ for the frequency f. To recognize the frequency f_{target} of the SSVEPs, CCA calculates the canonical correlation between the multi-channel EEG signals and the template at each stimulus frequency f ($f = f_1, f_2, \cdots, f_K$). As shown in equation (3), the frequency of the reference signals with the maximal correlation is selected as the frequency of SSVEPs.

$$f_{\text{target}} = \underset{f}{\text{argmax}}\, \rho(f), f = f_1, f_2, \cdots, f_K \quad (3)$$

Remark 1. Here, N_h is set to be two, i.e. the fundamental and second harmonics of SSVEP are used in the template. The optimal N_h may be different depending on different data lengths and noise issues. Searching for an optimal N_h is beyond the scope of this paper.

Remark 2. CCA has achieved great success in SSVEP BCIs. One important reason is probably the 'smart' choice of the template $Y(f)$, as a set of sine and cosine signals could well capture the frequency features of SSVEPs. Note that CCA could also get access to the phase information of SSVEPs by learning an effective weight vector w_y when the data length is long, e.g. the first two coefficients in w_y corresponding to $\cos(2\pi fn)$ and $\sin(2\pi fn)$ actually reflect the phase information of the fundamental component. However, with short data lengths, due to interference from the spontaneous EEG, CCA cannot capture the phase information of SSVEPs accurately.

In frequency-phase coding SSVEP BCIs, both the frequency and phase information are important for target identification. As discussed above, CCA cannot work well when the data length is short. To address this problem, the key is building a more robust template that contains the prior frequency and phase information. Nakanishi *et al* [17] and Chen *et al* [14] proposed to use the average of multiple trials from individual training data as the template and incorporate it with the standard CCA method. The proposed methods achieved significant accuracy improvement in comparison with the standard CCA method. However, a time-consuming training stage before operating BCIs is required. To facilitate the system use, a method that can build SSVEP templates without relying on individual training data is desired.

2.2. The proposed training-free framework for target identification

The proposed new framework was based on the assumption that a labeled dataset with multiple subjects (named source subjects) was available. The key idea to take advantage of the exiting source subjects' dataset to generate useful EEG templates (name transferred EEG templates) for a new subject (named a target subject) to capture frequency and phase information of SSVEP, i.e. transferring the useful information from source subjects to target subjects. Under this framework, a transfer template CCA (tt-CCA) method was first developed at the single-channel level; subsequently, it was generalized to multi-channel conditions, and finally, an online transfer template (ott-CCA) method was further proposed to enable online adaptation.

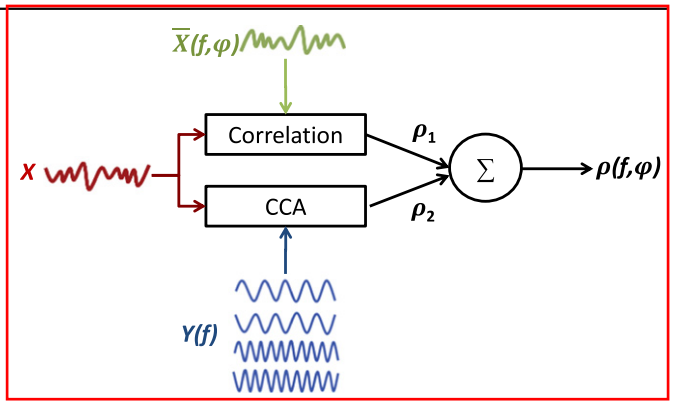

Figure 1. The proposed tt-CCA in single-channel level. X denotes the one-channel EEG of a new subject (i.e. the target subject), $Y(f)$ denotes the template used in the standard CCA methods, i.e. sine and cosine signals at frequency f. $\bar{X}(f, \varphi)$ denotes a transferred EEG template for one target encoded with frequency f and phase φ obtained by averaging the same channel EEG across many other subjects (i.e. source subjects). Here 'correlation' denotes the Pearson correlation analysis, and ρ_1 is the Pearson correlation coefficient. CCA denotes the canonical correlation analysis, and ρ_2 is the canonical correlation coefficient calculated using equation (2). The final $\rho(f, \varphi)$ is the sum of ρ_1 and ρ_2.

2.2.1. Single-channel level. In this section, we aimed to utilize the existing source subjects' dataset to generate transferred EEG templates for the target subject at the single-channel level. First, for each target encoded with frequency f and phase φ, a transferred EEG template $\bar{X}(f, \varphi)$ was generated by grand averaging the same channel EEG across source subjects. $\bar{X}(f, \varphi)$ can be viewed as the approximation to the target subject's real EEG template. Subsequently, as illustrated in figure 1, an approach incorporating $\bar{X}(f, \varphi)$ and CCA was used for target identification. As in the single-channel case, a natural way of utilizing $\bar{X}(f, \varphi)$ to identify targets is calculating Pearson correlation coefficient ρ_1 to access the similarity between EEG data X and transferred EEG template $\bar{X}(f, \varphi)$. In addition, it has been found that, in frequency-phase coding SSVEP BCIs, CCA could still contribute to detecting frequency components [17]. Thus, the canonical correlation coefficient ρ_2 was also calculated using CCA. Note that CCA can be implemented in the single-channel (one-dimension) case, as it has no requirements for the dimensions of two datasets. The sum of ρ_1 and ρ_2 is used as the feature for target identification. As in equation (3), the frequency and phase corresponding to the maximal $\rho(f, \varphi)$ is selected as the frequency and phase of the target's SSVEPs.

Remark 3. By calculating the Pearson correlation coefficient, both the frequency and phase information can

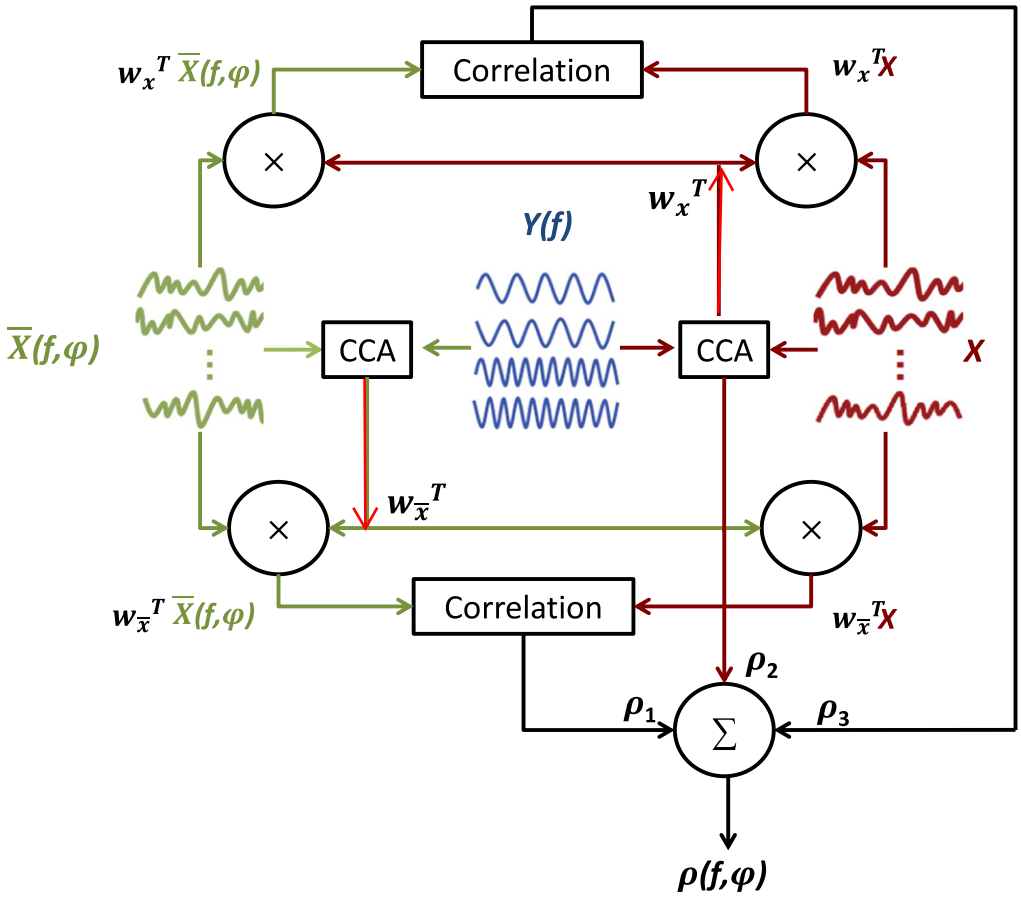

Figure 2. The proposed tt-CCA method in the multi-channel condition. X denotes the multi-channel EEG of the target subject, $Y(f)$ denotes the template used in the standard CCA methods, i.e. sine and cosine signals at frequency f. $\bar{\mathrm{X}}(f, \varphi)$ denotes a transferred EEG template for one target encoded with frequency f and phase φ got by averaging multi-channel EEG across source subjects. $w_{\dot{x}}^T$ and w_x^T are the transposes of the weight vectors for $\bar{\mathrm{X}}(f, \varphi)$ and X, respectively from standard CCA. 'Correlation' denotes the Pearson correlation analysis. ρ_1 is the Pearson correlation coefficient between two projected signals $w_{\dot{x}}^T \bar{\mathrm{X}}(f, \varphi)$ and $w_{\dot{x}}^T X$. Similarly, ρ_3 is the Pearson correlation coefficient between two projected signals $w_x^T \bar{\mathrm{X}}(f, \varphi)$ and $w_x^T X$. CCA denotes the canonical correlation analysis, and ρ_2 is the canonical correlation coefficient calculated using equation (2). The final $\rho(f, \varphi)$ is the sum of ρ_1, ρ_2 and ρ_3.

be captured; thus it is a simple yet efficient way to use transferred EEG template. In addition, $\rho(f, \varphi)$ is defined as the weighted sum of ρ_1 and ρ_2. Searching for the optimal weights of ρ_1 and ρ_2 is beyond the scope of this paper, and could be studied in future.

2.2.2. Multi-channel condition. In this section, we further generalize the proposed tt-CCA method to the multi-channel condition.

Similar to the single-channel level, first, for each target encoded with frequency f and phase φ, a multi-channel transferred EEG template $\bar{\mathrm{X}}(f, \varphi)$ was generated by averaging SSVEPs across source subjects. Note that the same channels were selected for source subjects and the target subject. $\bar{\mathrm{X}}(f, \varphi)$ can be viewed as the approximation of the target subject's real EEG template.

Subsequently, as illustrated in figure 2, an approach incorporating $\bar{\mathrm{X}}(f, \varphi)$ and CCA was used for target identification. Different from the single-channel case, the multi-channel character enables us to explore more information from the spatial (or channel) domain. Inspired by [14, 17], we first learned a direction vector $w_{\dot{x}}{}^T$ that maximized the SNR of $\bar{\mathrm{X}}(f, \varphi)$ at frequency f by implementing CCA with the datasets $\bar{\mathrm{X}}(f, \varphi)$ and $Y(f)$ (see figure 2). Also, a direction vector $w_x{}^T$ that maximized the SNR of the test EEG data X at frequency f was learned by implementing standard CCA with the datasets X and $Y(f)$. After that, both $\bar{\mathrm{X}}(f, \varphi)$ and X were projected onto these two directions for correlation analysis. Pearson correlation coefficients ρ_1 and ρ_3 were calculated to assess the similarity of the two dataset projections on these two directions respectively. In addition, ρ_2 was calculated using the standard CCA. The sum of ρ_1, ρ_2 and ρ_3 was taken as the final measurement of the similarity ($\rho(f, \varphi)$) between X and $\bar{\mathrm{X}}(f, \varphi)$. As in equation (3), the frequency and phase corresponding to the maximal similarity $\rho(f, \varphi)$ is selected as the frequency and phase of the target's SSVEPs.

Remark 4. Note that a large number of calculations could be completed before online implementation (e.g. the transferred EEG template $\bar{X}(f, \varphi)$, the weight vector $w_{\dot{x}}^T$, and the

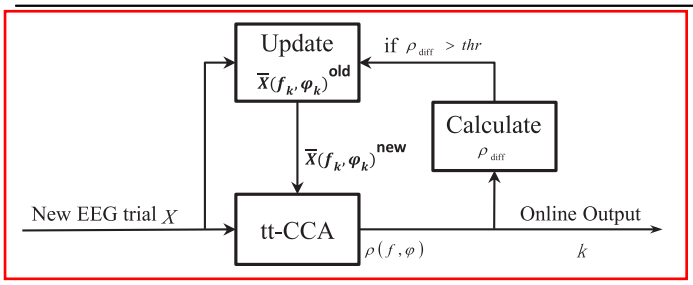

Figure 3. The procedure of the ott-CCA method. X indicates a new coming EEG trial. $\rho(f, \varphi)$ is a set of correlation values calculated by tt-CCA for all the candidate targets. k is the index of the recognized target (encoded with (f_k, φ_k)) which has the largest value of $\rho(f, \varphi)$ $\cdot\rho_{\text{diff}}$ is the difference between the first and the second largest values of $\rho(f, \varphi)$. *thr* is the threshold parameter used for determining whether or not to enable the updating operation. $\bar{X}(f_k, \varphi_k)^{\text{old}}$ and $\bar{X}(f_k, \varphi_k)^{\text{new}}$ are old and new templates for the current target encoded with (f_k, φ_k). Please refer to the following text for more details regarding the ott-CCA method.

projects $w_x^T \bar{X}(f, \varphi)$). During online calculation, compared with the standard CCA, the only extra computation loads are $w_x^T X$, $w_x^T \bar{X}(f, \varphi)$, and two Pearson correlation coefficient calculations. Therefore, the method can be implemented efficiently in online applications.

2.2.3. Online adaptation strategy. Based on the proposed tt-CCA method, in this section, we further propose an online adaptation strategy to take advantage of the individuals' data during online operation. The online transfer template method (ott-CCA for short) can update the transferred EEG templates gradually. The brief procedure of the proposed ott-CCA method is illustrated in figure 3.

The detailed steps of the ott-CCA method are as follows:

Step 1: Given a new test trial X, implement the tt-CCA method. Find the first and the second largest $\rho(f, \varphi)$ among all the candidate targets.

Step 2: Calculate the difference ρ_{diff} between the first and the second largest values of $\rho(f, \varphi)$. (The bigger the difference, the higher probability of the correct identification of the target.)

Step 3: If ρ_{diff} is above a pre-specified threshold *thr*, update the EEG template through equation (4). Otherwise, go back to step 1.

$$\bar{X}(f_k, \varphi_k)^{\text{new}} = \frac{1}{1 + n_k^{\text{old}}}\left(n_k^{\text{old}} * \bar{X}(f_k, \varphi_k)^{\text{old}} + X\right); \quad n_k^{\text{new}} = n_k^{\text{old}} + 1 \tag{4}$$

where X is a new coming test trial; $\bar{X}(f_k, \varphi_k)^{\text{old}}$ and $\bar{X}(f_k, \varphi_k)^{\text{new}}$ are old and new templates for the current target encoded with (f_k, φ_k); n_k^{old} and n_k^{new} are the number of the trials that have been used to get the averaged template of target (f_k, φ_k) before and after updating. All n_k ($k = 1, 2, \ldots K$) are initialized as c_0.

Step 4: Calculate a new direction w_x^T (see figure 2) that maximizes the SNR of $\bar{X}(f_k, \varphi_k)^{\text{new}}$ by implementing CCA with the datasets $\bar{X}(f_k, \varphi_k)^{\text{new}}$ and $Y(f)$.

Note that there is a tradeoff for the choice of parameters (*thr* and c_0) regarding to the performance of ott-CCA. In subsection 4.3, we reported the results of the ott-CCA method when choosing the following parameter settings: *thr* equals 0 (i.e. keep updating all the time) and c_0 equals the number of source subjects. We will further discuss the issues of parameters settings in the discussion section (see 5.2).

Remark 5. The online adaptation strategy benefits the proposed ott-CCA method from two aspects: first, it narrows the gap between a transferred EEG template $\bar{X}(f, \varphi)$ generated from source subjects and a real EEG template of the target subjects gradually; second, it catches up with the non-stationary changes of the target subject's EEG during the online operation. In addition, besides the proposed method in this paper, the proposed online adaptation strategy could also be used in other methods involving an EEG template for target identification in SSVEP BCIs.

3. Experiments

3.1. Experimental paradigms

The proposed method was evaluated in an offline joint frequency-phase coding SSVEP BCI experiment (one kind of hybrid frequency-phase coding SSVEP BCIs [14]). In the BCI system, the sampled sinusoidal stimulation method was used to generate stimulus signals with flexible frequencies and phases [14, 16, 37]. One advantage of this method is that the stimulus signal at any frequency (up to half of the screen refresh rate) and phase can be obtained. The results of our previous studies have proven the robustness of the sampled sinusoidal stimulation method in generating stimulus signals for eliciting SSVEPs [14, 16]. Targets are tagged with different frequencies and different phases. A total number of $N_x \times N_y$ targets (N_x rows, N_y columns) from a stimulus matrix are tagged with linearly increasing frequencies and phases. As illustrated in equation (5), the increments are proportional to the tar get index (from 1 to$N_x \times N_y$):

$$f(n_x, n_y) = f_0 + \Delta f \times \left[\left(n_y - 1\right) \times N_x + \left(n_x - 1\right)\right];$$
$$\varphi(n_x, n_y) = \varphi_0 + \Delta\varphi \times \left[\left(n_y - 1\right) \times N_x + \left(n_x - 1\right)\right] \tag{5}$$

In equation (5), f_0 and φ_0 indicate frequency and phase for the first target. Δf and $\Delta\varphi$ indicate the frequency and phase interval between two adjacent stimuli. In the BCI system, the user interface is a 5×8 stimulus matrix containing 40 characters (10 digits, 26 English letters and four other symbols). 40 frequencies (8–15.8 Hz with a 0.2 Hz interval) were used and the phase interval between two adjacent frequencies was 0.5π (i.e. $N_x = 5$, $N_y = 8$, $f_0 = 8$ Hz, $\varphi_0 = 0$, $\Delta f = 0.2$ Hz, $\Delta\varphi = 0.5\pi$). Stimuli were presented on a 23.6 in. LCD screen with a resolution of 1920×1080 pixels using a 60 Hz refresh rate. Each stimulus was presented

within a 140 × 140 pixel square and the distance between two adjacent stimuli was 50 pixels. For more details about the BCI system, please refer to [14].

3.2. Data acquisition

Twelve healthy subjects (8 females, aged 22–29 years) with normal or corrected-to-normal vision participated in the experiment. All participants were asked to read and sign an informed consent form before participating in the experiment.

EEG data were acquired using a Synamps2 system (Neuroscan, Inc.) with a sampling rate of 1000 Hz. Nine electrodes (Pz, PO5, PO3, POz, PO4, PO6, O1, Oz, and O2) were placed over parietal and occipital areas according to the international 10–20 system. The reference electrode was placed at the vertex. Electrode impedances were kept below 10 kΩ. During the experiment, subjects were seated in a comfortable chair in a dimly lit soundproof room at a viewing distance of approximately 70 cm from the monitor.

For each subject, the experiment consisted of 6 blocks. Each block contained 40 trials corresponding to all 40 targets indicated in a random order. Thus, each subject had a total of 240 (6 × 40) trials (6 trials per target). Each trial lasted 6 s. Each trial began with a visual cue (a red square) indicating a target stimulus. Subjects were asked to shift their gaze to the target as soon as possible within 0.5 s. After the cue offset, all 40 stimuli started to flicker for 5 s concurrently. Following the stimulus offset, the screen was blank for 0.5 s before the next trial began. To facilitate visual fixation, a red triangle appeared below the flickering target during the stimulation period. Note that the stimuli were shut off during the gaze shifting time. Switching off stimuli can avoid the unnecessary stimulus to subjects' eyes during the time of gaze shifting. Compared to successive stimulation, this paradigm may facilitate target detection by reducing eye fatigue and evoking more robust SSVEPs.

3.3. Experimental evaluations

Note that in this study, we focused on the method that can be applied in the situations when no training dataset of the target subject was available. We implemented tt-CCA for single-channel (Oz) and multi-channel (nine-electrode) conditions on the dataset collected in the above BCI experiment and compared them with the standard CCA method. To validate the effect of the online adaptation strategy, we took each subject's 240 trials of data as a sequential trial stream on the timeline, and simulated the ott-CCA method, i.e. after recognizing each trial, the current trial was used for updating the templates. The updated templates would be used for recognizing the next trial. The performance of ott-CCA and tt-CCA were also compared.

Specifically, we used a leave-one-out strategy to implement our methods. We sequentially left one of the 12 subjects out as the target subject, and the remaining 11 subjects were treated as source subjects. For each target tagged with $(f,\ \varphi)$, the labeled EEG of all the source subjects (totally $6 \times 11 = 66$ trials) were averaged to get a transferred EEG template $\bar{X}(f, \varphi)$ for the target subject. The average recognition accuracy across all the target subjects was used to indicate the performances of the method at a given time-window length. Eight data lengths ranging from 500 ms to 4000 ms with an interval of 500 ms were evaluated. For each target subject, the accuracies for all time lengths were also calculated using the standard CCA method for comparison. In the standard CCA method, the fundamental and second harmonics were used in the template, i.e. N_h was selected to 2 (see remark 1). Note that before implementing the proposed methods and the standard CCA method, no other preprocessing (e.g. data interception, filtering) procedure was involved. Although these preprocesses may further improve the recognition accuracy, this is beyond the scope of this study.

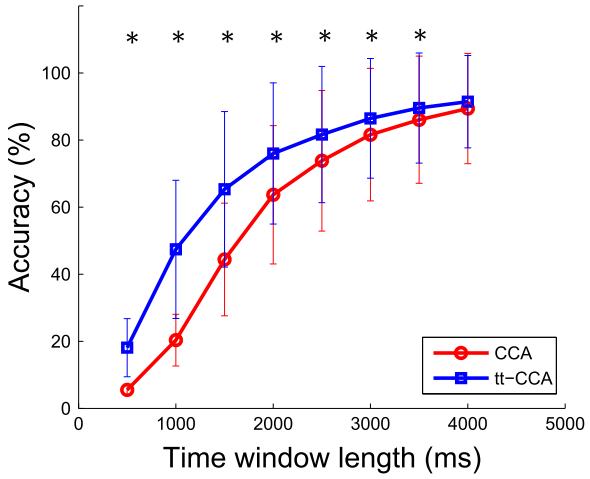

Figure 4. The accuracies across different time-window lengths using the standard CCA method and the tt-CCA method in the single-channel case. *indicates the statistical significant differences (paired t-test, $p < 0.05$).

4. Results

4.1. Single-channel level

The average accuracies across different time-window lengths using standard CCA and the proposed tt-CCA method on a single-channel level are illustrated in figure 4 (note that, as there are 40 targets, the chance-level accuracy is 2.5% (1/40)). Obviously, the proposed tt-CCA method outperforms CCA at all time-window lengths (* indicates the statistical significant differences, paired t-test, $p < 0.05$). The improvement is more significant when the time-window length is in the short range (e.g. less than 2 s).

To see more details of the results obtained with short data lengths (less than 2 s), the improved classification accuracies of all the subjects at short time-window lengths ($T = 0.5$ s, 1 s, 1.5 s, 2 s) are listed in table 1. Compared with CCA, the average accuracy was enhanced by 12.57%, 27.05%, 20.94% and 12.29% respectively when the time-window length is 0.5 s, 1 s, 1.5 s and 2 s using the proposed tt-CCA method. Note that the accuracies for all the subjects were improved,

Table 1. Improvements (%) (using tt-CCA compared with CCA) of all the subjects at short time window lengths ($T = 0.5$ s, 1 s, 1.5 s, 2 s) in single-channel (Oz) case.

Subjects	$T = 0.5$ s	$T = 1$ s	$T = 1.5$ s	$T = 2$ s
S1	14.58	31.25	25.42	16.25
S2	6.25	17.92	15.00	15.83
S3	28.75	47.50	20.00	1.67
S4	11.67	20.83	19.58	15.00
S5	13.33	18.75	18.33	9.58
S6	20.00	43.75	30.83	13.75
S7	3.75	9.58	5.00	2.08
S8	2.08	8.33	7.50	10.00
S9	10.83	26.67	31.67	21.25
S10	10.00	31.67	24.17	18.75
S11	7.08	19.17	15.42	8.75
S12	22.50	49.17	38.33	14.58
Average	**12.57 ± 7.91**	**27.05 ± 13.93**	**20.94 ± 9.80**	**12.29 ± 6.08**

Table 2. Improvements (%) (using tt-CCA compared with CCA) of all the subjects at short time-window lengths ($T = 0.5$ s, 1 s, 1.5 s, 2 s) in multi-channel condition.

Subjects	$T = 0.5$ s	$T = 1$ s	$T = 1.5$ s	$T = 2$ s
S1	16.67	42.92	21.67	9.17
S2	9.17	24.17	18.33	7.50
S3	35.00	32.92	4.17	0.83
S4	14.17	40.42	35.83	26.25
S5	8.33	14.58	3.75	−2.92
S6	13.33	30.83	13.33	−1.25
S7	7.92	39.17	21.67	6.25
S8	9.17	27.92	19.17	4.17
S9	12.08	48.75	54.58	30.83
S10	11.25	45.83	24.58	10.00
S11	17.50	17.08	2.92	−1.25
S12	22.50	20.00	5.42	−0.42
Average	**14.76 ± 7.71**	**32.05 ± 11.53**	**18.78 ± 15.14**	**7.43 ± 10.81**

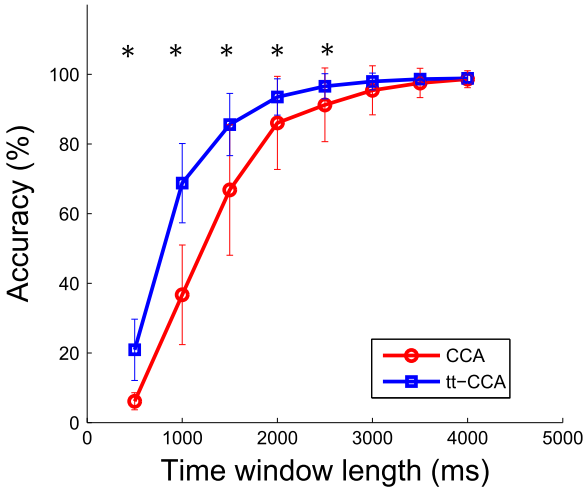

Figure 5. The accuracies across different time-window lengths using the standard CCA method and the tt-CCA method in the multi-channel condition. * indicates the statistical significant differences (paired t-test, $p < 0.05$).

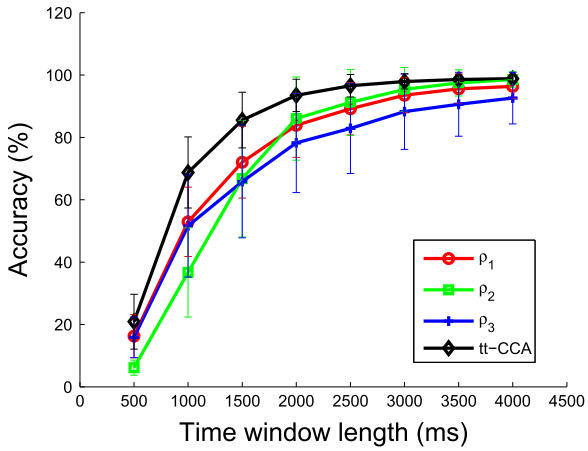

Figure 6. The accuracies across different time window lengths using ρ_1, ρ_2 (i.e. standard CCA), ρ_3 and tt-CCA ($\rho_1 + \rho_2 + \rho_3$) as classification criteria respectively in the multi-channel case.

with the maximal improvement being 49.17% (see S12, $T = 1$ s). Taken together, these results in the single-channel case clearly proved the efficiency of the transferred template in SSVEP identification.

4.2. Multi-channel condition

For the multi-channel condition, the average accuracies across different time-window lengths using standard CCA and the proposed tt-CCA method were illustrated in figure 5. The proposed tt-CCA method outperforms CCA especially with short time-window lengths. The differences are statistical significant at time-window lengths of 0.5 s, 1 s, 1.5 s, 2 s and 2.5 s (* indicates the statistical significant differences, paired t-test, $p < 0.05$).

To see more details of the results obtained with short data lengths (less than 2 s), the improved classification accuracies of all the subjects at short time-window lengths ($T = 0.5$ s, 1 s, 1.5 s, 2 s) are listed in table 2. Compared with CCA, the average accuracy was enhanced by 14.76%, 32.05%, 18.78% and 7.43% respectively when the time-window length is 0.5 s, 1 s, 1.5 s and 2 s using the proposed tt-CCA method. Also, the accuracies for most of the subjects were enhanced, with the maximal improvement of 54.58% (see S9, $T = 1.5$ s). In summary, the results in the multi-channel condition are consistent with those in the single-channel case, which clearly proved the efficiency of the proposed tt-CCA method.

As described in section 2.2.2, the classification criterion of the proposed tt-CCA method is the sum of three values: ρ_1, ρ_2 and ρ_3. ρ_2 is the canonical correlation coefficient calculated using the standard CCA. ρ_1 and ρ_3 are the Pearson correlation coefficients between the projections of test data and the transferred EEG template on two directions. To see the contributions from each part of the tt-CCA method, the accuracies using these three coefficients as classification criteria were calculated respectively.

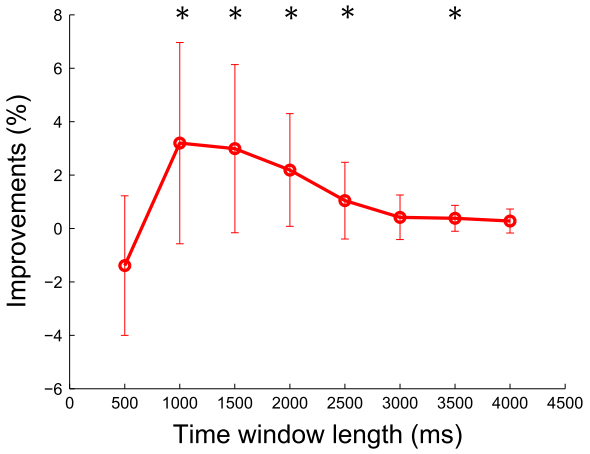

Figure 7. The improvements (enhanced accuracies) across different time-window lengths using ott-CCA, compared with tt-CCA. * indicates the statistical significant time window lengths (paired *t*-test, $p < 0.05$).

Table 3. Improvements (%) (using ott-CCA compared with tt-CCA) of all the subjects at short time-window lengths ($T = 0.5$ s, 1 s, 1.5 s, 2 s).

Subjects	$T = 0.5$ s	$T = 1$ s	$T = 1.5$ s	$T = 2$ s
S1	−0.42	7.50	0.83	1.67
S2	3.33	4.17	4.58	1.25
S3	−0.42	1.67	0.83	0.00
S4	−5.42	2.92	3.75	3.75
S5	−0.83	0.83	8.75	7.50
S6	1.67	5.42	3.33	2.50
S7	−1.67	2.92	6.67	4.17
S8	0.00	10.00	5.00	2.08
S9	−2.50	−2.92	−2.92	0.42
S10	−3.75	−2.50	0.00	0.83
S11	−1.25	5.83	3.33	1.67
S12	−5.42	2.50	1.67	0.42
Average	**−1.39 ± 2.61**	**3.19 ± 3.77**	**2.99 ± 3.15**	**2.19 ± 2.11**

As shown in figure 6, consistent with our previous analysis, the standard CCA method (corresponding to ρ_2) does not perform well with short data (say less than 2 s). However, using the information from the transferred EEG template, the classification accuracies based on ρ_1 and ρ_3 are much better than CCA in the short time-window lengths. Therefore, the improvements in short data lengths are due to the additional information provided by transferred EEG templates. In addition, the classification methods based on ρ_1 and ρ_3 also perform well with long time-window lengths. As illustrated in figure 6, by combining ρ_1, ρ_2 and ρ_3, tt-CCA could largely improve the performance of CCA at a short time range and also slightly improve the performance at a long time range.

4.3. Simulated test of online adaptation

To validate the effect of online adaptation, we calculated the classification accuracies using ott-CCA to compare with tt-CCA in the multi-channel condition. The average improvements across different time-window lengths are illustrated in figure 7. It turned out that ott-CCA significantly improved tt-CCA at 1 s, 1.5 s, 2 s, 2.5 s and 3.5 s time-window lengths (as illustrated in figure 7. * indicates the statistical significant differences, paired *t*-test, $p < 0.05$).

The improvements are more significant in the short time range (except 0.5 s). Compared with the long time-window lengths, which showed high accuracy, the classification accuracies with short time lengths have larger room for improvement using the online adaptation strategy.

To see more details of the results obtained with short data lengths (less than 2 s), the improved accuracies of all the subjects at short time-window lengths ($T = 0.5$ s, 1 s, 1.5 s, 2 s) are listed in table 3. Compared with tt-CCA, the average accuracy was further enhanced by 3.19%, 2.99% and 2.19% respectively when the time-window length is 1 s, 1.5 s and 2 s using ott-CCA. These results proved the efficiency of the proposed online adaptation strategy. However, the failure of ott-CCA with the 0.5 s data length suggested that the ott-CCA method is actually based on the tt-CCA method. Hence, the ott-CCA method will not work well when the classification accuracy obtained by tt-CCA is too low (e.g. around 20% with 0.5 s data; see figure 5).

5. Discussions

5.1. The benefits from transferred EEG templates in tt-CCA

The proposed tt-CCA method significantly outperformed the standard CCA method. It is very important to answer the question of why the transferred EEG templates are useful for new target subjects. We further made the following theoretical analysis on the characters of the transferred EEG templates.

First, for each target, averaging the data with the same label across source subjects is a frequency preserving operation. Considering a specific stimulus frequency of a target, the SSVEPs of each subject can be viewed as an approximated simple harmonic motion (here we only consider the fundamental harmonics). Although the phases of the source subjects' SSVEPs are not exactly the same because of individual variation of visual latencies in the visual system [15, 38, 39], according to the superposition principle of simple harmonic motions, averaging these SSVEPs with the same frequency and different phases will result in an EEG template containing the same frequency. This is important, as it enables the possibility of using transferred EEG templates to approximate target subjects' real EEG templates. Also, it enables the use of the standard CCA method to find the optimal directions (i.e. spatial filters) of the transferred EEG templates to maximize the SNR of the SSVEPs.

Second, for each target, the latency from averaged templates across source subjects can be viewed as an estimation of target subjects' visual latencies. Normally, under the same stimulus paradigm, the variability of SSVEP latencies across subjects is relatively small compared with the periods of the stimuli [15, 17, 38, 39], which will result in relatively small

phase differences across subjects. According to the superposition principle of simple harmonic motions, averaging SSVEPs with the same frequency and small phase differences will result in an EEG template containing SSVEPs with the same frequency and a new phase which can be viewed as the mean of all the source subjects' phases. Basically, we are using this phase (or latency) to approximate that of the target subjects. This is a good estimation if no additional prior information is available. From a statistical point of view, this operation usually ensures a minimum expectation loss. We further implemented the following analysis to validate the assumptions above.

The visual latencies across subjects were estimated using the method described in [17, 38, 39]. It was found that the averaged latency was 142 ± 16 ms, which was consistent with the results reported in [17, 38, 39]. The latency variation between subjects was relatively small compared with the stimulus period (e.g. 8 Hz: 125 ms, 15.8 Hz: 63.3 ms), which ensured that in most cases the phases difference between the transferred templates and a target subject's real templates would be in an acceptable range (e.g. less than π).

To see, on average, whether the templates averaged from all source subjects are better approximations than the templates chosen from individual source subjects, we compared the spatial–temporal similarities (note that each template of a target is a matrix) between these two types of templates and target subjects' individual (or real) templates respectively. We applied the same approach used in the tt-CCA method to calculate similarities between any two templates, i.e., to first apply standard CCA to each template to learn the optimal directions that maximize the SNR of SSVEPs; then, two correlation coefficients between the projections of two templates on these two optimal directions were calculated respectively; finally, the mean of the two correlation coefficients was taken as the final correlation coefficient of these two templates. For a target subject (say subject T), using this method and data length at 1.5 s, we calculated the correlation coefficients between the corresponding individual templates of the target subject and each one of the source subjects (i.e. $\bar{\mathrm{X}}_T(f_k, \varphi_k)$ and $\bar{\mathrm{X}}_s(f_k, \varphi_k)$, $k = 1,\ldots 40$, $s = 1,\ldots T-1, T+1,\ldots 12$), resulting in a set of correlation coefficients $\{\mathrm{r}_{Tsk}\}$. Also, the corresponding correlation coefficients between the target subject's individual templates and the target subject's transferred templates (generated by averaging the data across all the source subjects, denoted as $\bar{\mathrm{X}}_{TS}(f_k, \varphi_k)$) were calculated, resulting in a set of correlation coefficients $\{\mathrm{r}_{TSk}\}$. Then, we averaged $\{\mathrm{r}_{Tsk}\}$ and $\{\mathrm{r}_{TSk}\}$ across all the source and target subjects, resulting in two correlation vectors $\bar{\mathrm{r}}_s$ and $\bar{\mathrm{r}}_S$ ($\bar{\mathrm{r}}_s$, $\bar{\mathrm{r}}_S \in \mathbb{R}^{40\times 1}$) respectively. It turned out that the values in $\bar{\mathrm{r}}_s$ were significantly smaller than the corresponding values in $\bar{\mathrm{r}}_S$ (0.3260 ± 0.045 versus 0.4958 ± 0.066, paired t-test, $p = 2.6\mathrm{e}-30$), which proved that, on average, the templates averaged across all the source subjects are a better approximation than the templates chosen from an individual source subject. Note that for individual source subjects, it is actually possible that the templates from some subjects are better than the transferred template averaged across all the source subjects. However, on average, when no prior information is available, the averaged transferred template will be a better choice.

To see whether the approximated templates are good enough for target identification, for a target subject (say subject T), we calculated the correlation coefficients between any two templates in a target subject's individual template set and the transferred EEG templates set (i.e. the correlation between $\bar{\mathrm{X}}_T(f_{k1}, \varphi_{k1})$ and $\bar{\mathrm{X}}_{TS}(f_{k2}, \varphi_{k2})$, $k1 = 1,\ldots 40$, $k2 = 1,\ldots 40$), resulting in a correlation coefficients matrix R_{TS} (with size 40×40, $R_{TS}(k1, k2) = r_{TSk1k2}$). To better understand this analysis, as an example, three correlation matrices (R_{TS} as well as the other two matrices, i.e. R_{TT}: a correlation coefficient matrix for the target subject's individual templates set; and R_{Ts}: a correlation coefficient matrix for the target subject's individual templates set and one of the source subjects' individual templates set (here S2)) for target subject S1 were calculated and are illustrated in figure 8. The following observations can be found. In R_{TS}, the key observation was that most of the diagonal elements are the maximum elements in the rows of the correlation coefficient matrix, which ensured that, among the 40 candidates in transferred EEG templates set, the target subjects' data is closest to the one whose label is the same. Although the values of the diagonal elements in R_{TS} are smaller than those in R_{TT}, they are obviously larger than those in R_{Ts}. These observations proved the efficiency of the transferred templates.

In a word, the above analysis proved that the averaged template is a good approximation to the target subjects' individual template. In addition, by applying ott-CCA, as time goes on, the averaged template could be adjusted gradually toward better approximations of the target subjects' real template. As we pointed out above, it is actually possible that the template of one source subject is better than the transferred template averaged across multiple source subjects as long as we have additional prior information about the structures of target subjects' data, which inspires more efficient online updating strategies in ott-CCA.

5.2. The parameters settings of ott-CCA

In subsection 4.3, we reported the results of ott-CCA under the following parameters settings: $thr = 0$ and $c_0 = 11$. Actually, there is a tradeoff for the choices of threshold thr and c_0 regarding to the performance in ott-CCA. thr controls the number of trials that can be used to update templates. c_0 can be viewed as the initial number of virtual trials of target subjects' EEG data X. It balances the relative importance of the original template and the current data. Given smaller thr and c_0, one trial will have larger possibility and weight to update the transferred EEG templates, enabling fast updating. However, at the same time, it suffers a higher risk of incorrectly assigning the test data to EEG templates, leading to worse templates. This happens especially when the classification accuracy is low. For instance, the failure of online updating at 0.5 s (see figure 7) may be due to the low classification accuracy using the tt-CCA method and small chosen

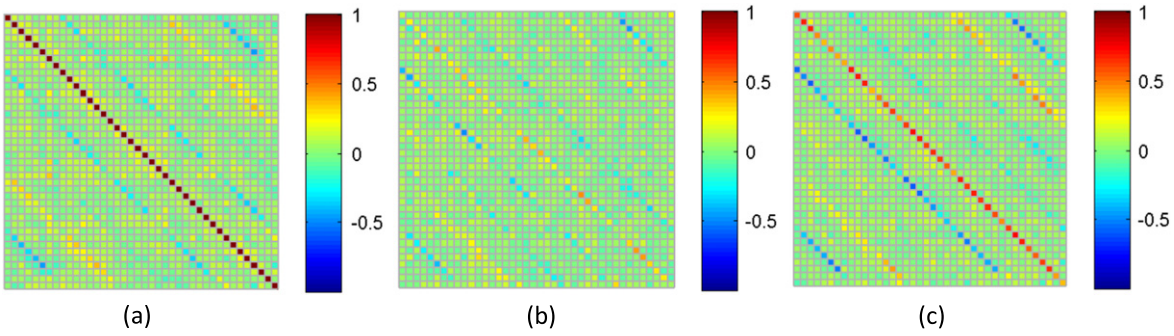

Figure 8. Correlation coefficient matrices for (a) the target subject's individual templates set R_{TT}. (b) The target subject's individual template set and one of the source subjects' individual template sets (here S2) R_{Ts}, and (c) the target subjects' individual template set and the transferred EEG templates set R_{TS}. The element in the $k1$th row and $k2$th column of the matrixes indicates the correlation coefficient between the template for the $k1$th target and the template for the $k2$th target.

Table 4. Improvements (%) using ott-CCA compared with tt-CCA with 1.5 s data across different parameters.

thr	c_0				
	1	11	22	33	66
0	2.40	2.99	2.12	2.05	1.01
0.1	2.85	2.71	2.12	1.88	1.11
0.2	2.57	1.81	1.49	1.25	0.97
0.3	1.81	1.25	1.01	0.52	0.38
0.4	1.25	0.66	0.49	0.17	0.14
0.5	0.38	0.49	0.10	0.07	0.10
1	0.00	−0.03	0.00	−0.03	−0.07

values of *thr* and c_0 (*thr* = 0, c_0 = 11). However, if we could get a relatively high accuracy using the tt-CCA method, then smaller *thr* and c_0, which enable fast updating, may make ott-CCA more efficient.

To confirm the above ideas, we calculated the improvements between tt-CCA and ott-CCA with 1.5 s data using different *thr* (*thr* = 0, 0.1, 0.2, 0.3, 0.4, 0.5, 1) and c_0 (c_0 = 1, 11, 22, 33, 66). The results are listed in table 4. We can see that the improvements are more significant when the parameters are in a range of small values. This is consistent with our expectations. As we discussed above, with relatively high accuracy (based on the tt-CCA method, we could get an accuracy around 85%), smaller values of *thr* and c_0 should be chosen. Also, we can see that in most cases of parameters settings, the ott-CCA method will enhance the performance of tt-CCA and that the performance of ott-CCA is not very sensitive to the change of parameters as long as the parameters change smoothly. This means that even if we do not give much consideration to parameter settings, ott-CCA will still work well in most cases.

In practice, the parameters could be determined via leave-one-out cross validation on the existing subjects' dataset. Specifically, we could sequentially leave one of the existing subjects out as the target subject, and implement the ott-CCA method with various parameter settings. The parameter settings corresponding to the maximum average accuracy across all the subjects could be chosen as the final parameter settings.

5.3. An open framework

The proposed methods constitute an open framework. Overall, the proposed framework of methods consisted of two parts. One is the transferred EEG template-based correlation analysis (termed the transferred EEG template part), and the other is standard CCA (termed the CCA part). Any methods that can improve one of the two parts can be involved in the proposed framework to further improve its performance. For instance, to improve the transferred EEG template part, as the label information is available for source subjects, the multiset canonical correlation analysis (M-CCA) and common feature analysis (CFA) methods proposed in [40, 41] can be applied to learn more robust and useful frequency and phase features. Also, to improve the CCA part, the recently proposed methods in [42, 43] can be involved to improve the frequency detection ability of CCA by properly handling background EEG-related problems. In addition, more theoretical analyses and issues on the further optimization and generalization of methods are still open for future study.

6. Conclusion

In summary, a new training-free framework for target detection was proposed for frequency-phase coding SSVEP BCIs in this paper. Combined with CCA, EEG templates from the existing source subjects were used for enhancing SSVEP detection for new target subjects. Under this framework, a tt-CCA method at single-channel and multi-channel conditions was developed and an ott-CCA method was further proposed to enable the online adaptation of transferred templates. The efficiency of the proposed framework was proved in a simulated SSVEP BCI study using a joint frequency-phase coding method. More importantly, this study also sheds light on the benefits of exploring and exploiting the existing subjects' information to naive users in EEG-based BCIs.

Acknowledgments

This work is supported by the National Natural Science Foundation of China (61431007), the National Basic Research Program (973) of China (2011 CB933204) and Chinese 863 Project: 2012AA011601.

Reference

[1] Birbaumer N, Ghanayim N, Hinterberger T, Iversen I, Kotchoubey B, Kübler A, Perelmouter J, Taub E and Flor H 1999 A spelling device for the paralyzed *Nature* **398** 297–8

[2] Wang Y, Gao X, Hong B, Jia C and Gao S 2008 Brain–computer interfaces based on visual evoked potentials: feasibility of practical system design *IEEE Eng. Med. Biol. Mag.* **27** 64–71

[3] Bin G, Gao X, Wang Y, Hong B and Gao S 2009 Research frontier: VEP-based brain–computer interfaces: time, frequency, and code modulations *IEEE Comput. Intell. Mag.* **4** 22–6

[4] Middendorf M, McMillan G, Calhoun G and Jones K S 2000 Brain–computer interfaces based on the steady-state visual-evoked response *IEEE Trans. Rehabil. Eng.* **8** 211–4

[5] Cheng M, Gao X, Gao S and Xu D 2002 Design and implementation of a brain–computer interface with high transfer rates *IEEE Trans. Biomed. Eng.* **49** 1181–6

[6] Wang Y, Wang R, Gao X, Hong B and Gao S 2006 A practical VEP-based brain–computer interface *IEEE Trans. Neural Syst. Rehabil. Eng.* **14** 234–40

[7] Bin G, Gao X, Yan Z, Hong B and Gao S 2009 An online multi-channel SSVEP-based brain–computer interface using a canonical correlation analysis method *J. Neural Eng.* **6** 046002

[8] Gao S, Wang Y, Gao X and Hong B 2014 Visual and auditory brain–computer interfaces *IEEE Trans. Biomed. Eng.* **61** 1435–47

[9] Gollee H, Volosyak I, McLachlan A J, Hunt K J and Graser A 2010 An SSVEP-based brain–computer interface for the control of functional electrical stimulation *IEEE Trans. Biomed. Eng.* **57** 1847–55

[10] Ortner R, Allison B Z, Korisek G, Gaggl H and Pfurtscheller G 2011 An SSVEP BCI to control a hand orthosis for persons with tetraplegia *IEEE Trans. Neural Syst. Rehabil. Eng.* **19** 1–5

[11] Diez P F, Mut V A, Perona E M A and Leber E L 2011 Asynchronous BCI control using high-frequency SSVEP *J. Neuroeng. Rehabil.* **8** 39

[12] Khalona R A, Atkin G E and LoCicero J L 1993 On the performance of a hybrid frequency and phase shift keying modulation technique *IEEE Trans. Commun.* **41** 655–9

[13] Yongacoglu A and Li W 1997 Hybrid permutation frequency phase modulation *Proc. Can. Conf. on Electron. Comput. Eng.* pp 197–200

[14] Chen X, Wang Y, Nakanishi M, Jung T P and Gao X 2014 Hybrid frequency and phase coding for a high-speed SSVEP-based BCI speller *Proc. 36th Ann. Int. IEEE Conf. Engineering in Medicine and Biology Society (EMBC)* pp 3993–6

[15] Jia C, Gao X, Hong B and Gao S 2011 Frequency and phase mixed coding in SSVEP-based brain–computer interface *IEEE Trans. Biomed. Eng.* **58** 200–6

[16] Chen X, Chen Z, Gao S and Gao X 2014 A high-ITR SSVEP-based BCI speller *Brain–Computer Interfaces* **1(3-4)** 181–91

[17] Nakanishi M, Wang Y, Wang Y T, Mitsukura Y and Jung T P 2014 A high-speed brain speller using steady-state visual evoked potentials *Int. J. Neural Syst.* **24** 1–18

[18] Lin Z, Zhang C, Wu W and Gao X 2006 Frequency recognition based on canonical correlation analysis for SSVEP-based BCIs *IEEE Trans. Biomed. Eng.* **53** 2610–4

[19] Chang M H, Baek H J, Lee S M and Park K S 2014 An amplitude-modulated visual stimulation for reducing eye fatigue in SSVEP-based brain–computer interfaces *Clin. Neurophysiol.* **125** 1380–91

[20] Wu Z, Lai Y, Xia Y, Wu D and Yao D 2008 Stimulator selection in SSVEP-based BCI *Med. Eng. & Phys.* **30** 1079–88

[21] Cao T, Wan F, Wong C M, da Cruz J N and Hu Y 2014 Objective evaluation of fatigue by EEG spectral analysis in steady-state visual evoked potential-based brain–computer interfaces *Biomed. Eng. Online* **13** 28

[22] Punsawad Y and Wongsawat Y 2012 Motion visual stimulus for SSVEP-based BCI system *Proc. Ann. Int. IEEE Conf. Engineering in Medicine and Biology Society (EMBC)* pp 3837–40

[23] Yin E, Zhou Z, Jiang J, Yu Y and Hu D 2014 A dynamically optimized SSVEP brain–computer interface (BCI) speller *IEEE Trans. Biomedical Eng.* doi:10.1109/TBME.2014.2320948

[24] da Cruz J N, Wan F, Wong C M and Cao T 2015 Adaptive time-window length based on online performance measurement in SSVEP-based BCIs *Neurocomputing* **149** 93–9

[25] Jin J, Allison B Z, Sellers E W, Brunner C, Horki P, Wang X and Neuper C 2011 An adaptive P300-based control system *J. Neural Eng.* **8** 036006

[26] Millán J R and Mourino J 2003 Asynchronous BCI and local neural classifiers: An overview of the adaptive brain interface project *IEEE Trans Neural. Syst. Rehabil. Eng.* **11** 159–61

[27] Samek W, Meinecke F C and Muller K R 2013 Transferring subspaces between subjects in brain–computer interfacing *IEEE Trans. Biomed. Eng.* **60** 2289–98

[28] Tu W and Sun S 2012 A subject transfer framework for EEG classification *Neurocomputing* **82** 109–16

[29] Kang H and Choi S 2011 Bayesian multi-task learning for common spatial patterns *Proc. IEEE Int. Workshop on Pattern Recognition in NeuroImaging (PRNI)* pp 61–4

[30] Kang H, Nam Y and Choi S 2009 Composite common spatial pattern for subject-to-subject transfer *IEEE Signal Process. Lett.* **16** 683–6

[31] Heger D, Putze F, Herff C and Schultz T 2013 Subject-to-subject transfer for CSP-based BCIs: Feature space transformation and decision-level fusion *Proc. 35th Ann. Int. IEEE Conf. Engineering in Medicine and Biology Society (EMBC)* pp 5614–7

[32] Kindermans P J, Tangermann M, Müller K R and Schrauwen B 2014 Integrating dynamic stopping, transfer learning and language models in an adaptive zero-training ERP speller *J. Neural Eng.* **11** 035005

[33] Wang Y and Jung T P 2011 A collaborative brain–computer interface for improving human performance *PLoS One* **6** e20422

[34] Yuan P, Wang Y, Wu W, Xu H, Gao X and Gao S 2012 Study on an online collaborative BCI to accelerate response to visual targets *Proc. Ann. Int. IEEE Conf. Engineering in Medicine and Biology Society (EMBC)* pp 1736–9

[35] Yuan P, Wang Y, Gao X, Jung T P and Gao S 2013 A collaborative brain–computer interface for accelerating human decision making *Universal Access in Human–Computer Interaction. Design Methods, Tools, and Interaction Techniques for Einclusion* (Berlin: Springer) pp 672–81

[36] Hotelling H 1936 Relations between two sets of variates *Biometrika* **28** 321–77

[37] Manyakov N V, Chumerin N, Robben A, Combaz A, van Vliet M and Van Hulle M M 2013 Sampled sinusoidal

stimulation profile and multichannel fuzzy logic classification for monitor-based phase-coded SSVEP brain–computer interfacing *J. Neural Eng.* **10** 036011

[38] Pan J, Gao X, Duan F, Yan Z and Gao S 2011 Enhancing the classification accuracy of steady-state visual evoked potential-based brain–computer interfaces using phase constrained canonical correlation analysis *J. Neural Eng.* **8** 036027

[39] Russo F D and Spinelli D 1999 Electrophysiological evidence for an early attentional mechanism in visual processing in humans *Vision Res.* **39** 2975–85

[40] Zhang Y, Zhou G, Jin J, Wang X and Cichocki A 2014 Frequency recognition in SSVEP-based BCI using multiset canonical correlation analysis *Int. J. Neural Syst.* **24** 1450013

[41] Zhang Y, Zhou G, Jin J, Wang X and Cichocki A 2014 SSVEP recognition using common feature analysis in brain–computer interface *J. Neurosci. Methods* **244** 8–15

[42] Wei C S, Lin Y P, Wang Y, Wand Y T and Jung T P 2013 Detection of steady-state visual-evoked potential using differential canonical correlation analysis *Proc. 6th IEEE EMBS Ann. Int. Conf. Neural Eng.* pp 57–60

[43] Nakanishi M, Wang Y, Wang Y T, Mitsukura Y and Jung T P 2014 Enhancing unsupervised canonical correlation analysis-based frequency detection of SSVEPs by incorporating background EEG *Proc. 36th Ann. Int. IEEE Conf. Engineering in Medicine and Biology Society (EMBC)* pp 3053–6